THE ASTROPHYSICAL JOURNAL, 355:617–626, 1990 June 1

LB 1800: A BRIGHT ECLIPSING CATACLYSMIC VARIABLE AND A TRANSIENT X-RAY SOURCE

D. A. H. BUCKLEY,[1,2] D. J. SULLIVAN,[1,3] R. A. REMILLARD,[4] I. R. TUOHY,[1] AND M. CLARK[5]
Received 1989 July 27; accepted 1989 December 6

ABSTRACT

The star LB 1800 has been discovered to be a 13th mag high-excitation cataclysmic variable exhibiting nova-like characteristics and partial eclipses in its light curve. It has subsequently been identified as the optical counterpart of the transient hard X-ray source 4U 0608−49 following analysis of *HEAO 1* data. Both the radial velocity and photometric variations have a period of 5.56 hr, while the K-velocity of the relatively uncomplicated radial velocity curves is 134 ± 9 km s^{-1}, leading to a mass function of $5.8 \pm 0.3 \times 10^{-2}\ M_\odot$. The dynamical and eclipse solutions point to an orbital inclination of $87° \pm 3°$ and a mass ratio of 0.46 ± 0.04 for the empirical secondary mass $0.55\ M_\odot$. The implied white dwarf mass is therefore quite high at $\sim 1.2\ M_\odot$. We estimate the disk size, from timings of first and last contact, to be very close to that of the secondary star. Phase-dependent, double-peak emission lines are sometimes observed. We argue that the orbital variations in the relative strengths of the red and blue peaks arise from changing hot-spot visibility. Also we contend that the double peaks may be a result of an absorption self-reversal. Such an interpretation is supported by the observed wavelength dependence of this reversal in the Balmer lines, and we note that the maximum depth of this central reversal, and the maximum strength of Ca II H and K absorption, occurs at the orbital phase ($\sim$0.8–0.9) when the cool accretion stream is seen projected against the bright disk. In many respects LB 1800 resembles other high-excitation eclipsing nova-like systems (e.g., SW Sex, V1315 Aql, and DW UMa), although it appears to be more easily understood in terms of the canonical model for a cataclysmic variable.

Subject headings: stars: dwarf novae — stars: eclipsing binaries — stars: individual (LB 1800) — X-rays: binaries

I. INTRODUCTION

Eclipsing cataclysmic variables (hereafter CVs) can in principle provide a knowledge of the stellar dimensions (masses, radii) and measures of the size and structure of the accretion disks (e.g., Sulkanen, Brasure, and Patterson 1981; Horne 1985). In some cases the light curves can be deconvolved into the eclipses of the individual components: the white dwarf, accretion disk, and disk hot spot (e.g., Warner and Cropper 1983; Penning *et al.* 1984; Wood, Irwin, and Pringle 1985), which may then lead to estimates of their dimensions (e.g., Cook and Warner 1984). With the addition of time-resolved spectroscopic observations, a dynamical solution for the binary system may be achieved (e.g., Kaitchuck, Honeycutt, and Schlegel 1983; Penning *et al.* 1984; Downes *et al.* 1986; Shafter, Hessman, and Zhang 1988). In addition, the continuum and emission-line eclipses may yield information on the spatial distribution of the relevant emission regions. For example, the high-excitation region, characterized by He II λ4686 emission, is often centrally located in the disk (Downes *et al.* 1986; Watts *et al.* 1986), or an optically thin region of line emission may exist above the disk plane near the inner regions of the disk (Honeycutt, Schlegel, and Kaitchuck 1986). In recent times much effort has gone into deriving the intensity, and hence temperature, distributions in accretion disks using Horne's (1985) maximum entropy disk image reconstruction technique (Horne and Steining 1985; O'Donoghue, Fairall, and Warner 1987; Warner and O'Donoghue 1987, 1988). An alternative method of fitting synthetic eclipse curves to observations has also been used (Zhang, Robinson, and Nather 1986.

Approximately 26 eclipsing CVs have so far been identified (Ritter 1984; Warner and Cropper 1983; Downes *et al.* 1986), of which about half have been detected as X-ray sources. Among the entire sample of CVs observed by the *Einstein* satellite, 70% were found to be X-ray emitters (Patterson and Raymond 1985) at some level.

X-ray emission characteristics of CVs are dependent on the specific accretion regime involved. Important distinctions are evident depending upon the strength of the magnetic field of the accreting white dwarf, namely weak ($B < 1$ MG) and strong ($B > 10$ MG) field systems. In the former case, the accretion disk is thought to extend all the way to the surface of the white dwarf, where a boundary layer is formed and the kinetic energy of the accreting matter is released via shocks (Pringle and Savonije 1979) or viscous dissipation (Tylenda 1981). Some gas in this region expands above the disk plane, forming an optically thin corona, which cools by thermal bremsstrahlung with a characteristic temperature of 5–8 keV (Córdova and Mason 1984). The hard X-ray properties (e.g., Mason 1985) and the correlation of X-ray and optical parameters (Patterson and Raymond 1985) support the above model for systems with low accretion rates ($\dot{M} \leq \sim 10^{16}$ g s^{-1}). For increased accretion rates, the cooling time scale is less than the time scale for adiabatic expansion, which results in heating of the disk material and surface layers of the white dwarf, which then radiate as blackbodies primarily in the EUV region (Córdova and Mason 1984; Mason 1985). Because of inefficiencies in producing a boundary layer corona, the total fraction of accretion energy released in hard X-ray (>2 keV) is

[1] Mount Stromlo and Siding Spring Observatories, Australian National University.
[2] Department of Astronomy, University of Cape Town.
[3] Physics Department, Victoria University of Wellington, New Zealand.
[4] Center for Space Research, Massachusetts Institute of Technology.
[5] Mount John University Observatory, Lake Tekapo, New Zealand.

quite low (Córdova and Mason 1984), leading to X-ray–to–optical luminosity ratios (L_x/L_{opt}) of ~ 1 for quiescent dwarf novae (low $\dot{M}$), and < 0.06 for dwarf novae in outburst (high $\dot{M}$). For CVs in which the magnetic field pressure overwhelms the gas ram pressure at some radial distance in the disk, the consequence may be a totally or partially disrupted disk. The gas is then channelled along field lines onto a confined region of the white dwarf's surface: its polecap, or rather "auroral" zone. The X-ray characteristic of these *magnetic variables*, which include the synchronously rotating polars (AM Her systems) and the asynchronous intermediate polars (DQ Her systems), are quite different from the weak field CVs. The magnetic systems exhibit hard ($kT > 10$ keV) bremsstrahlung emission, with $L_x/L_{opt} > 1$ and as high as 10.

In this paper we report the discovery of a bright eclipsing CV, which we identify as the optical counterpart to a transient X-ray source. While the optical characteristics are similar to other high-excitation nova-like CVs the gross X-ray and optical properties indicate a possible intermediate polar classification, though this will have to be confirmed. A spectroscopic and photometric study is undertaken in which we derive a dynamical solution for the system.

II. IDENTIFICATION AND X-RAY OBSERVATIONS

LB 1800 (Luyten and Anderson 1958; Fig. 1) was discovered serendipitously to be a cataclysmic variable following low-dispersion spectroscopy carried out with the 1.9 m reflector at Mount Stromlo Observatory on 1986 February 14. In Figure 2 we show the discovery spectrum of LB 1800; however, we

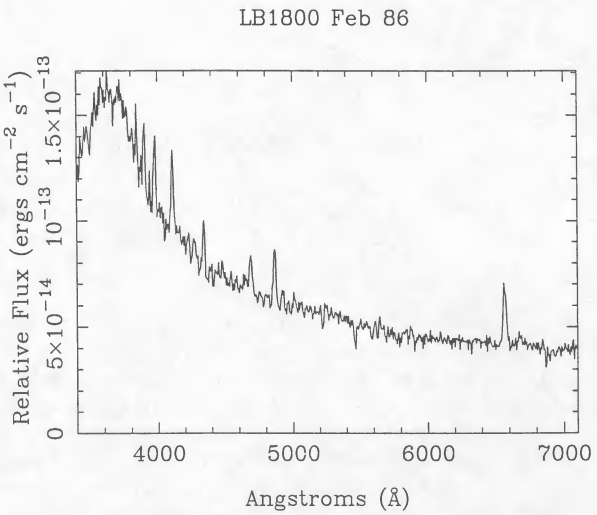

FIG. 2.—Discovery spectrum of LB 1800 (1986 February 14) taken with the MSO 1.9 m telescope and Cassegrain spectrograph using the photon counting array. The flux distribution in the blue is not accurate due to atmospheric dispersion and slit effects.

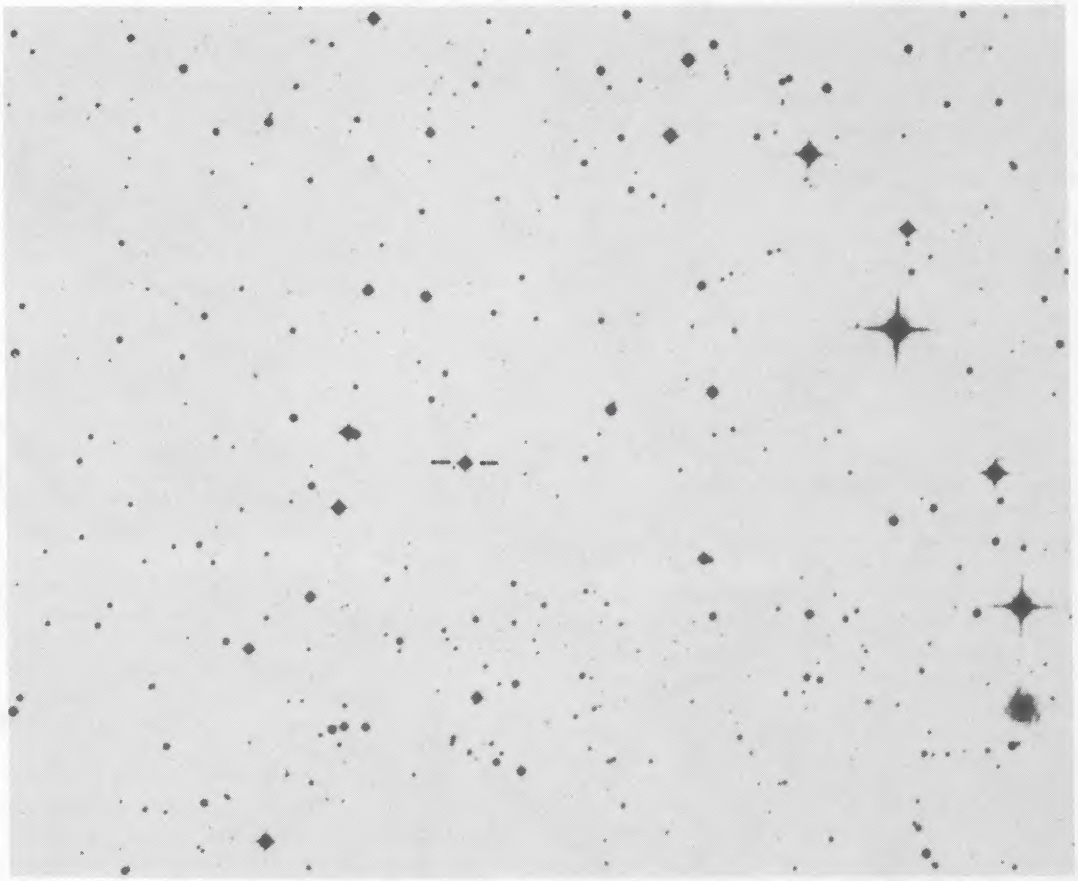

FIG. 1.—Finding chart for LB 1800 from the SRC-J survey. Approximate coordinates from the AAT (accurate to $\sim 2''$) are R.A. = $06^h09^m15^s.9$, decl. = $-48°43'45''$ (1950). The scale of the chart is $\sim 15' \times 12'$, with north up and east to the left.

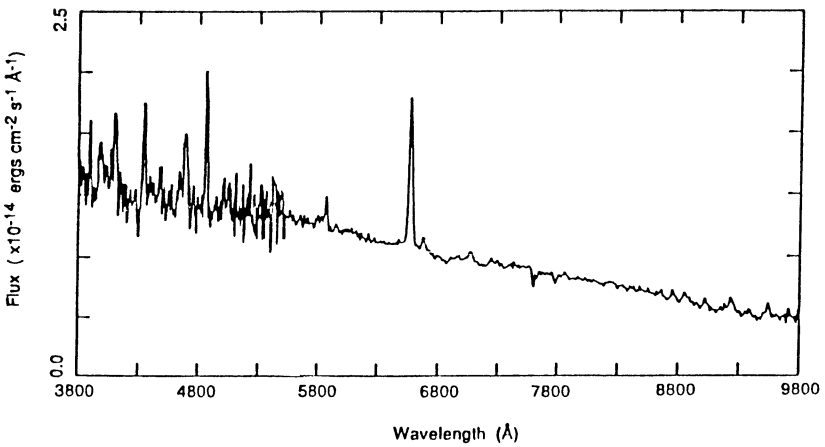

FIG. 3.—Combined blue and red spectrum of LB 1800 taken with the IPCS/FORS combination at the AAT on 1986 July 27

emphasize that the flux calibration in the blue ($\lambda < \sim 4400$ Å) is uncertain due to atmospheric dispersion effects. Another low-resolution spectrum of this object, extending the spectral coverage into the red ($\lambda \sim 10{,}000$ Å, $\Delta\lambda \sim 20$ Å), was obtained on 1986 July 27 using the 3.9 m Anglo-Australian Telescope (AAT) utilizing the RGO spectrograph with the imaging photon counting system (IPCS), plus the faint object red spectrograph (FORS). The spectra exhibit the typical characteristics of a CV, namely Balmer, He I, and He II emission lines on a blue continuum. Also evident in the red FORS spectrum are the Paschen lines. However, there appear to be no absorption features attributable to a cool secondary star, although we emphasize the lower resolution of the red spectrum (~ 20 Å). The combined IPCS/FORS spectrum for LB 1800 is shown in Figure 3, while the line fluxes and widths are given in Table 1. From our fluxed spectra we estimate the 5000–6000 Å continuum flux as $1.2 \pm 0.2 \times 10^{-11}$ ergs cm^{-2} s^{-1}.

The newly identified CV was found to be inside the error box of the previously unidentified *Uhuru* X-ray source 4U 0608−49 (Forman *et al.* 1978), whose 2–10 keV flux is 7.4×10^{-11} ergs cm^{-2} s^{-1}, assuming a Crab-like spectrum. The *HEAO 1* Large Area Sky Survey catalog (LASS; Wood *et al.* 1984), which represents a more sensitive view of the X-ray sky during the first all-sky celestial scan by *HEAO 1*, does not include a detection near the position for LB 1800 or 4U 0608−49. The 3 σ upper limit from the LASS experiment is approximately 1×10^{-11} ergs cm^{-2} s^{-1}, from which we conclude that 4U 0608−49 is a high-latitude ($b \sim 27°$) transient. We have investigated both the second and third celestial scans by *HEAO 1*, examining the observations by both the LASS and the Scanning Modulation Collimator (MC; Gursky *et al.* 1978) experiments. In each analysis, the source transits were superposed and fitted for a single pointlike X-ray source, as described by Remillard *et al.* (1986). During the second *HEAO 1* scan of the *Uhuru* position (1978 March 16–25), the X-ray source was again visible, with an estimated flux of 5×10^{-11} ergs cm^{-2} s^{-1} in the 2–10 keV band. The LASS detection has a statistical significance of ~ 5 σ, while the MC results are 2.8 σ and 3.4 σ in the two collimators over the full sensitivity range 1–13 keV. Figure 4 shows the *Uhuru* error box, the line of position derived from our analysis of the LASS observations during the second *HEAO 1* scan, and error diamonds produced by the intersection of the two collimator bands during the same scan. LB 1800 is located within each of these positional constraints, and as the probability for such a bright CV falling within these bounds by chance is negligible, we conclude that LB 1800 is the optical counterpart of a recurring X-ray transient.

Adopting the above X-ray and optical fluxes leads to a ratio of F_x(2–10 keV)/F_{opt}(5000–6000 Å) of ~ 4, although these were obviously not simultaneous measurements. This value is high

TABLE 1

LB 1800 EMISSION-LINE FLUXES AND WIDTHS

Line	Flux (ergs cm^{-2} s^{-1})	EW (Å)	σ (Å)
Hε	$7.3 \pm 0.8 \times 10^{-14}$	5.9 ± 0.6	5.5 ± 0.6
Hδ	$2.0 \pm 0.1 \times 10^{-13}$	16.2 ± 1.1	14.4 ± 1.0
Hγ	$1.5 \pm 0.1 \times 10^{-13}$	12.2 ± 0.7	9.3 ± 0.6
He I λ4471	$4.4 \pm 0.8 \times 10^{-14}$	3.6 ± 0.6	7.7 ± 1.5
C III/N III	$6.6 \pm 0.9 \times 10^{-14}$	5.7 ± 0.8	12.7 ± 2.0
He II λ4686	$1.9 \pm 0.1 \times 10^{-13}$	16.7 ± 0.9	14.4 ± 0.9
Hβ	$2.0 \pm 0.1 \times 10^{-13}$	17.0 ± 0.6	8.1 ± 0.3
Hα	$3.29 \pm 0.04 \times 10^{-13}$	35.9 ± 0.4	13.4 ± 0.2

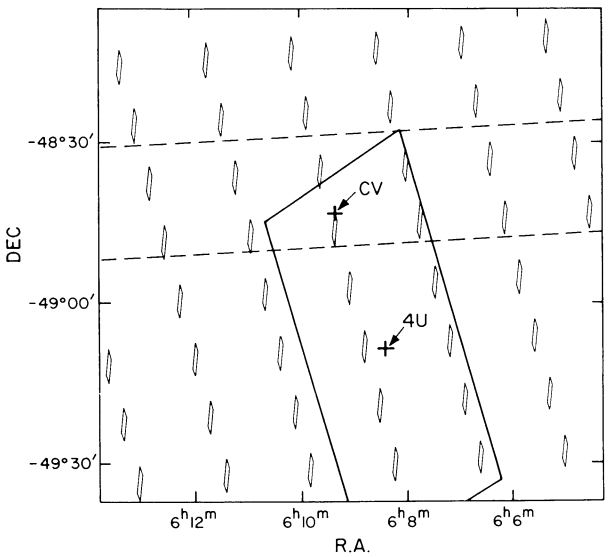

FIG. 4.—X-ray map for 4U 0608−49 derived from the *Uhuru* satellite (*trapezoid*) and *HEAO 1* LASS (*dashed lines*) and MC (*diamonds*) experiments. The position of LB 1800 is shown as "CV."

for a normal CV, although characteristic of a *magnetic* CV (Córdova and Mason 1984). Such a classification for LB 1800 is supported by the presence of strong He II λ4686 emission. A brief spectropolarimetric measurement of LB 1800 was conducted on the AAT on 1988 March 26 with the result that the star was shown not to be strongly polarized. The upper limit for circular polarization over the wavelength region ~3400 to 1.6 μm is <0.5%, thus ruling out classification of LB 1800 as a polar but still admitting the possibility that the star is an *intermediate* polar. Further discussion of this point is left for the conclusion (§ VII).

III. RADIAL VELOCITY MEASUREMENTS

Following the identification of LB 1800 as a new cataclysmic binary, time-resolved spectroscopy of the object was obtained at the first available opportunity. These observations were conducted on 1987 January 27 from 9 to 16.3 hours UT, using the Cassegrain spectrograph on the MSO 1.9 m telescope. Time-resolved spectra were obtained in the region λλ3937–5000 at a resolution of ~2.5 Å. The detector employed was the Mount Stromlo two-dimensional photon counting array (Stapinski, Rodgers, and Ellis 1981; Rodgers *et al.* 1988). The aim of these observations was to investigate the radial velocity and emission-line profile variations. The raw spectra were wavelength-calibrated using comparison arc spectra taken regularly (~every 40 minutes) during the course of the observations. Several methods were utilized in order to determine reliable velocities: the cross-correlation, Gaussian profile fitting, and Gaussian convolution techniques. The first of these methods estimated velocity shifts of *groups* of lines (e.g., the Balmer series. He I lines) relative to a high signal-to-noise ratio template spectrum, using the Tonry-Davis algorithm (Tonry and Davis 1977), where a parabola is fitted to the central peak of the cross-correlation function. The Balmer lines were studied as a single set, with the other lines being edited out of each spectrum and replaced by a local average of the continuum. The second technique derived velocity information of individual lines by fitting a Gaussian function to the lines, while the third method used is in essence the double Gaussian convolution scheme devised by Schneider and Young (1980). This technique has been used extensively (Shafter 1983, 1985; Shafter, Szkody, and Thorstensen 1986; Horne, Wade, and Szkody 1986) and gives reliable velocities from the line wings, considered to represent best the white dwarf orbital motion (e.g., Horne, Wade, and Szkody 1986).

In Figure 5 we present the radial velocity variations of the Balmer lines measured using the cross-correlation technique and include the least-squares single sine fit to the data. The choice of template had little effect upon the results. The best-fit sinusoid has a period of 5.34 ± 0.44 hr, a velocity semi-amplitude ($K_{\rm Balmer}$) of 134 ± 9 km s^{-1}, and zero phase, defined as superior conjunction of the white dwarf, occurring at 1987 January 27 12.86 ± 0.12 UT (HJD 2,446,823.0376 ± 0.0050). The period and zero phase were later found to be consistent with the more accurately determined photometric ephemeris (§ V). In particular we note that the observed time of superior conjunction of the white dwarf is within phase 0.03 ± 0.02 of the predicted minimum, extrapolated from our photometric ephemeris.

Once the orbital period was determined, all of the spectra were binned into 10 approximately equally spaced phase bins. These higher signal-to-noise ratio data were then reanalyzed using both the Gaussian profile–fitting technique and the wing-sensitive Gaussian filter algorithm. The results indicate that, surprisingly, the radial velocity curves show little complexity and are similar for different line species and different positions in the profile where the velocity determination is weighted. Specifically we found that the limits on variations in K and φ_0 were, respectively, ~20 km s^{-1} and ~0.05 for line wing positions between 600 and 1200 km s^{-1} of line center for Hβ. In Figure 6 the radial velocity variations are shown for the Hβ line, at positions in the line wings of 600, 900, and 1200 km s^{-1} from line center. The only variation seen is for the γ velocity.

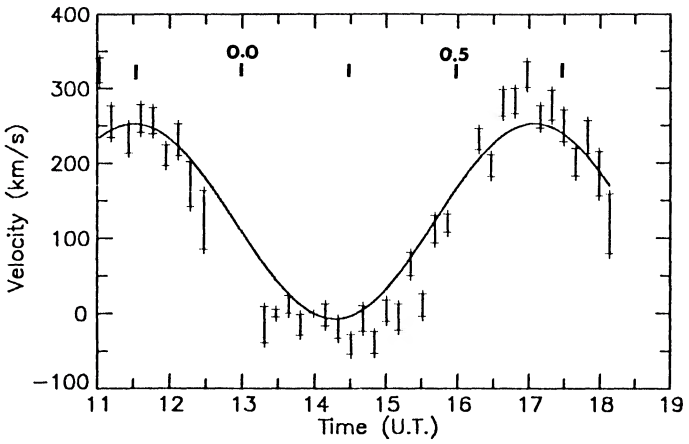

FIG. 5.—Radial velocity variations, as a function of universal time on 1987 January 27, of the Balmer lines derived using the cross-correlation method, together with the sinusoidal radial velocity curve fit. Photometric phases are indicated in the upper portion of the diagram.

IV. SPECTRAL LINE VARIATIONS

The structure of the emission lines themselves deserves some comment. While the lines do exhibit temporal variations in their structure, the persistent *symmetric* double-peaked structure, which typifies high-inclination CVs, is not obvious in our spectra. Phase-binned spectra for LB 1800 are presented in Figure 7. Lack of such structure has also been noted for the

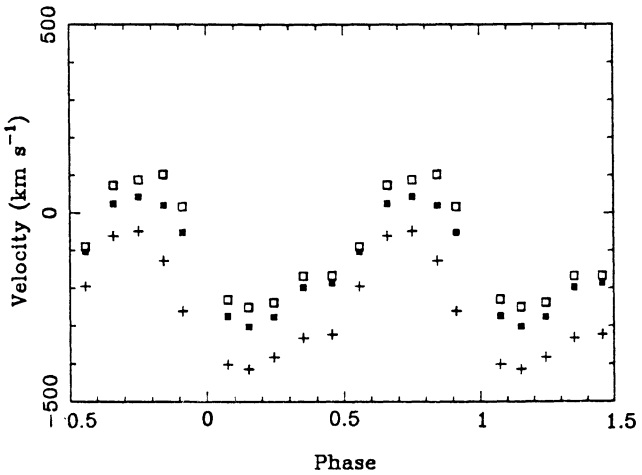

FIG. 6.—Radial velocity variations for Hβ line determined using the Gaussian convolution scheme at three positions in the line wings: 600 (*plus sign*), 900 (*filled squares*), and 1200 (*open squares*) km s^{-1} from line center. The velocities are plotted with respect to photometric phase, and two cycles are shown for clarity.

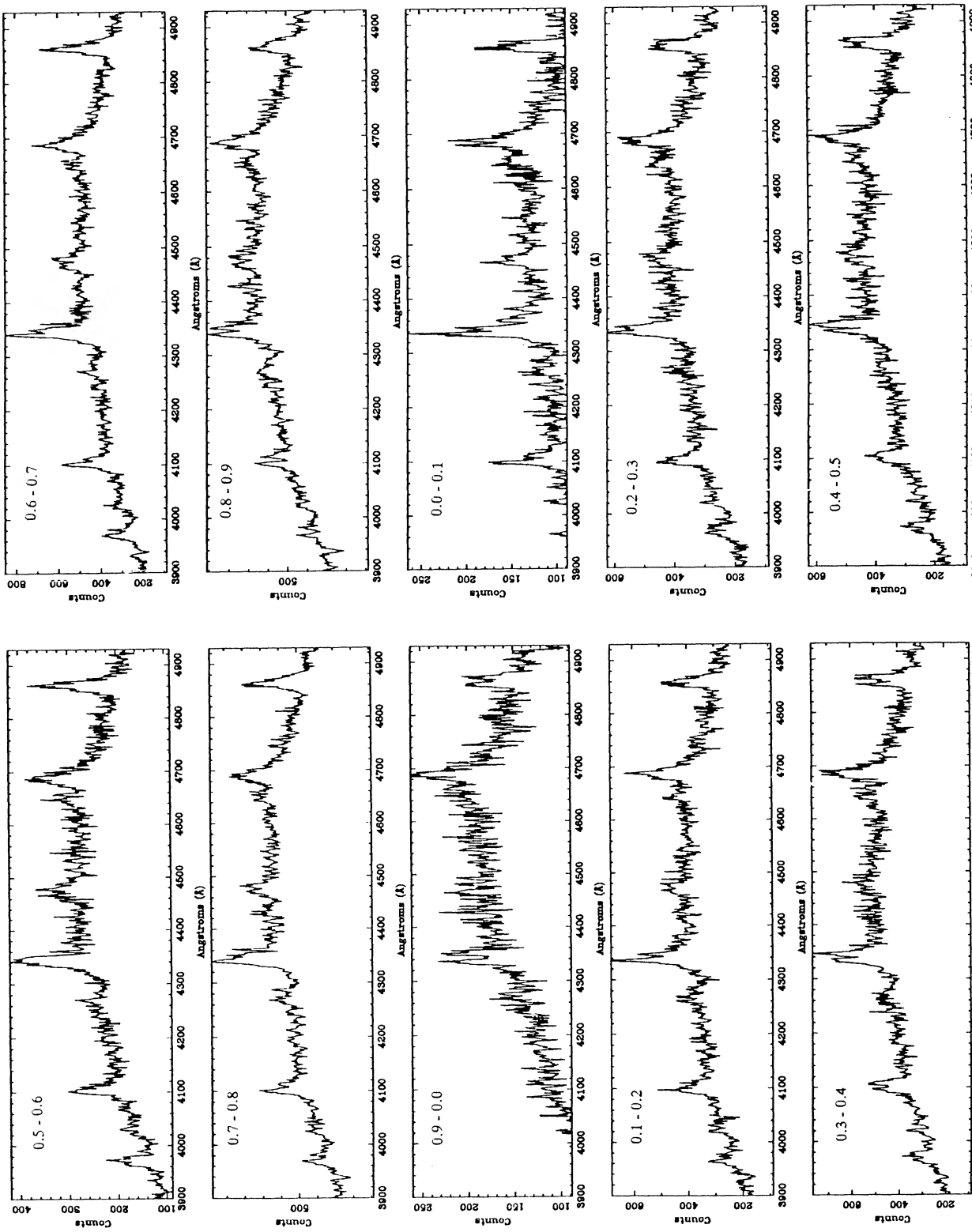

FIG. 7.—Phase-binned spectra of LB 1800 using the photometric ephemeris. Ten equally spaced photometric phase bins were used, with phase = 0.00 defined as photometric minimum.

high-excitation eclipsing nova-like system SW Sex (PG 1012−029; Honeycutt, Schlegel, and Kaitchuck 1986), as well as the absence of an s-wave. This is somewhat surprising since Penning *et al.* (1984) have shown that a hot spot is present in the system, contributing as much as 40% to the high-excitation emission lines and significantly (>20%) to the continuum. Double-peaked profiles are certainly seen in our spectra of LB 1800 at certain orbital phases, particularly near primary eclipse at phase 0.8–0.2. Also noticeable in some of the phase binned spectra is the variation in the strength of the red and blue peaks of the Balmer lines. Spectra in the phase interval 0.6–0.8 have the blue peak considerably stronger than the red peak, and possibly *vice versa* for the phase interval 0.3–0.4. Such a variation in emission peak strengths may be explained by the superposition of a third component, attributed to the disk hot spot at the accretion stream/disk interface. Intuitively this explanation seems acceptable for LB 1800, since the resulting s-wave would appear blueshifted with respect to the disk emission profile at phase ~0.6, where we view the hot spot moving directly toward us, while the projected accretion disk orbital velocity is redshifted. This situation might be expected to be reversed around $\phi \sim 0.1$, when the velocity of the hot-spot material is most positive, though the eclipse will still be affecting the hot spot's visibility. We also note just prior to eclipse ($\phi \sim 0.8$–0.0), when the hot spot is usually best observed in these systems, that the spectra show red and blue peaks of roughly equal strength. This is consistent with the dynamical condition whereby the hot spot material is moving transversely to our line of sight. It is far from clear, however, that the often observed double-peaked profiles are entirely a result of dynamical effects caused by pseudo-Keplerian disk rotation of accretion disk material. We note in several spectra, particularly in the phase range 0.8–0.9, that the dip between the red and blue emission peaks increase in depth toward the higher order Balmer series. Such a wavelength-dependent absorption reversal is characteristic of an opacity effect. This may explain the fact that the double-peaked structure is always more obvious in Hγ than in Hβ. Also coincident with the increasingly strong Balmer absorption reversal is the appearance of strong Ca II K λ3933 absorption, which may also explain the deep absorption core of Hϵ if it is due to the superposition of Ca II H λ3968. The fact that the Ca II K absorption is strongest in the same phase interval ($\phi \sim 0.8$–0.9) where the possibly wavelength-dependent reversals seen in the Balmer lines, Hϵ, Hδ, and Hγ, are strongest, is consistent with an absorption effect. This phase interval is near where the hot spot is best seen and also where the accretion stream is seen projected against the bright disk, and thus an increase in absorption-line strengths would be expected. We also note that in our fluxed lower resolution spectra, the Balmer decrement is relatively flat, with Hα/H$\beta \sim 1.7$, indicating high optical depths in the lines. In the above respects LB 1800 is reminiscent of V1315 Aql (KPD 1911+1212; Downes *et al.* 1986).

The variation of the emission-line parameters can in principle provide spatial information regarding the low- and high-excitation regions of the accretion disk in a CV. In many systems there is ample evidence, often dynamical, that the He II emission is produced in the inner disk regions. For example the complete disappearance of He II λ4686 and C III–N III $\lambda\lambda$4640–4650 in V1315 Aql during eclipse led Downes *et al.* (1986) to this very conclusion. They also showed that the increased equivalent widths of the lower excitation lines could be explained in terms of a more complete obscuring of the continuum region compared to the low excitation line-emitting region. In general, most accretion disk models have a more centrally confined, optically thick continuum emitting region in comparison to the more extended optically thin region. However, this has to some extent been contradicted by observations that indicate that the radial extent of the line region is less than for the continuum. For example, in SW Sex again, Honeycutt, Schlegel, and Kaitchuck (1986) have shown from observations of line intensity variations that the high- and low-excitation regions may be extended in the *vertical* direction (i.e., orthogonal to the disk), while still remaining centrally located. They invoke a bipolar wind model to explain this extension.

Our data show that the equivalent widths of both the He II λ4686 and Hβ lines are roughly constant over the orbital period, except for an increase immediately after the eclipse at ~13 hr UT (see Fig. 8). The rapid and deep eclipse ingress/egress precluded the taking of spectra during most of the eclipse, since LB 1800 fell below the threshold of the telescope TV guiding system. It is apparent, however, that the higher Balmer series (Hδ and Hϵ) all but disappear near phase zero. A comparison of the emission line and continuum eclipses (§ V) shows that both have approximately the same duration.

V. PHOTOMETRY

Following the spectroscopic identification of LB 1800 as a CV, a search for eclipses and other variability was undertaken during 1987 February, immediately after the spectroscopy. Photometry was obtained at two observing sites. Several nights of high-speed white-light photometry were obtained using the 0.6 m photometric telescope at Mount John University Observatory, New Zealand (MJUO). In addition, the ANU 2.3 m alt-azimuth advanced technology telescope (ATT) at Siding Spring Observatory (SSO) was used to conduct *UBVRI* photometry of LB 1800 on 1987 February 26. Data from both observing runs revealed the presence of deep eclipses, while the higher time resolution MJUO observations detected short time scale variability characteristic of a CV.

The MJUO observations were accomplished using the high-speed mode of a two-channel photometric system (van der Peet 1987). One of these channels was used to observe the target star (LB 1800), while the second channel monitored a constant comparison star. Both channels were operated in the

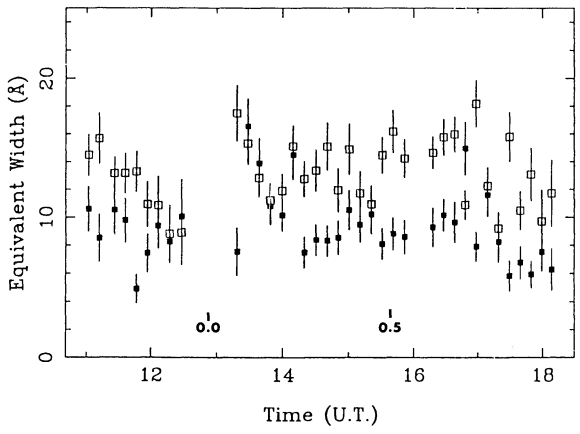

FIG. 8.—He II λ4686 (*filled squares*) and Hβ (*open squares*) equivalent width variations (in Å) on 1987 January 27. Universal times are plotted on the *x*-axis, and photometric minimum occurs at 12.86 hr UT.

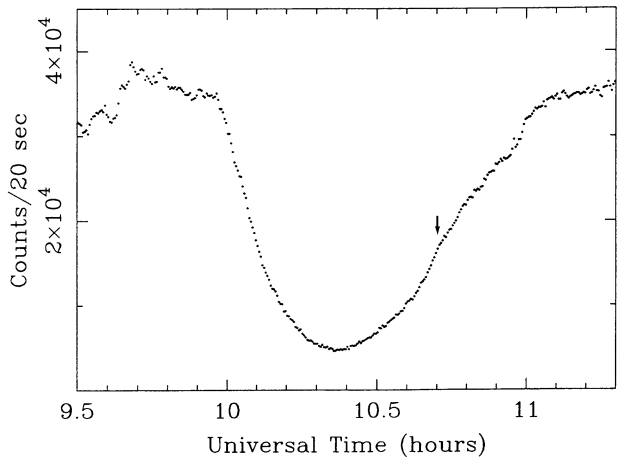

FIG. 9.—White-light eclipse light curve of LB 1800, plotted against universal time, observed on 1987 February 20 using the 0.6 m photometric telescope at MJUO. The arrow indicates the kink in the egress shoulder of the eclipse curve (see text).

photomultiplier-defined "white light," with an S20 tube used in the main channel. The system was run in a continuous mode with 5 s integrations, while the monitor channel was interrupted occasionally for guiding checks. Data obtained during a 3 hr run of photometric conditions on 1987 February 20, during which LB 1800 went into eclipse, are shown in Figure 9. The ordinate scale represents detected photons per 20 s integration. A deep eclipse, covering a time period of approximately 1 hr, is readily apparent. Low-level variability on a time scale of minutes (flickering) is also evident. This is particularly marked before the onset of the eclipse. Data from the second channel are not shown, but they confirmed both the photometric quality of the night and the reality of the flickering in LB 1800.

The SSO observations are displayed in Figure 10. These data were obtained using the single-channel SCAP photometer mounted at a Nasmyth focus of the ATT, and reductions to the standard system were effected in the usual way. As SCAP operates with a rapidly rotating filter wheel, the individual colors are accurately determined from contemporaneous integrations of the relevant two filters. The data show a deep eclipse, up to 3 mag in U, but are of lower time resolution than the MJUO data. In Table 2, we present colors and V magnitudes for two out-of-eclipse phase angles, before and after eclipse ($\phi \sim 0.91$ and 0.41), and at mid-eclipse. It is apparent that as the eclipse proceeds, the colors, except perhaps for $U-B$, become redder. This is consistent with the gradual occulting of a hotter body (the disk) by a cooler object (the secondary star). There is slight evidence, at the 2–3 σ level, for a sharp, brief decrease in U at mid-eclipse, manifested in $U-B$ data. This will need to be confirmed with higher time resolution data in the future. Another feature of the $U-B$ variations is the lower amplitude quasi-sinusoidal variation. Whether or not this is a permanent feature of the system will be resolved after future multicolor photometry.

All of the eclipse data, from both the SSO and MJUO observing sites, are very similar. Morphologically the eclipse light curves of LB 1800 resemble those of other nova-like variables, outbursting dwarf novae and old novae (e.g., Horne 1985), namely broad asymmetric wings and a rounded minimum. There is no evidence for rapid brightness variations during eclipse, as is often the case of quiescent dwarf novae, and has been attributed to the eclipse of the hot spot and the white dwarf. A maximum, or "hump," is often observed just before ingress, a common feature in the light curves of dwarf novae and some nova-like CVs. The onset of eclipse (i.e., first contact) is quite sudden and relatively easily measured, unlike many other systems whose eclipse wings gradually merge into the out-of-eclipse flickering. For each of the observed eclipses we have measured phase of first and last contact (ϕ_f) and the half-width of the eclipse at half-light ($\phi_{1/2}$), as a fraction of orbital phase. We derive values of $\phi_f = 0.105 \pm 0.005$ and $\phi_{1/2} = 0.052 \pm 0.002$. Another common feature in the data is the asymmetry of the eclipse curve and the apparent kink in the egress light curve (see arrow in Fig. 9). This is likely due to the multicomponent nature of the total luminosity of the system. In particular the asymmetric behavior is thought to be due to a secondary source of luminosity, over and above that of the accretion disk/white dwarf, and is presumably due to the disk hot spot, as in SW Sex (Penning *et al.* 1984).

The entire photometric data comprise nine eclipse observations, including the two light curves shown here. The times of minima, observed and calculated from the ephemeris discussed below, are given in Table 3. The times of minima were estimated graphically, and a linear ephemeris fitted using the initial spectroscopic period of 5.3 hr as a starting point. This ephemeris is given as

$$T_{\min}(\mathrm{HJD}) = 2{,}446{,}836.9620 \pm 0.0010 + 0.231928 \pm 0.000010E\,.$$

The ephemeris was used to phase all of the light curves and resulted in a mean white light–light eclipse curve, which was used in the analysis in the following section.

VI. MODEL AND DYNAMICAL SOLUTION

In this section we explore a likely dynamical model for LB 1800. We begin with the now standard CV model: a late spectral type, main-sequence secondary star, in a binary orbit with a white dwarf companion (the primary), is transferring material via Roche lobe overflow through the inner Lagrangian point to

TABLE 2

MAGNITUDES AND COLORS FOR LB 1800

MAG/COLOR	IN-ECLIPSE	OUT-OF-ECLIPSE	
	$\varphi = 0.0$	$\varphi = 0.41$	$\varphi = 0.91$
V	15.80	13.40	13.58
$U-B$	−0.40	−0.58	−0.60
$B-V$	0.95	0.16	0.30
$V-R$	0.83	0.25	0.35
$V-I$	1.70	0.60	0.70

TABLE 3

LB 1800 ECLIPSE TIMES

Date (1987)	HJD −2,440,000	$(O-C)$	Cycles	Phase Interval
Feb 9	6836.0379	0.0035	−4	0.88–0.50
Feb 10	6836.9621	0.0000	0	0.79–0.43
Feb 19	6846.0059	−0.0014	39	0.64–0.54
Feb 20	6846.9333	−0.0017	43	0.83–0.42
Feb 21	6848.0930	−0.0016	48	0.15–0.14
Feb 23	6849.9500	0.0000	56	0.97–0.85
Feb 25	6852.0373	−0.0001	65	0.64–0.04
Feb 26	6852.9651	0.0000	69	0.77–0.71
Feb 28	6855.0533	0.0011	78	0.21–0.20

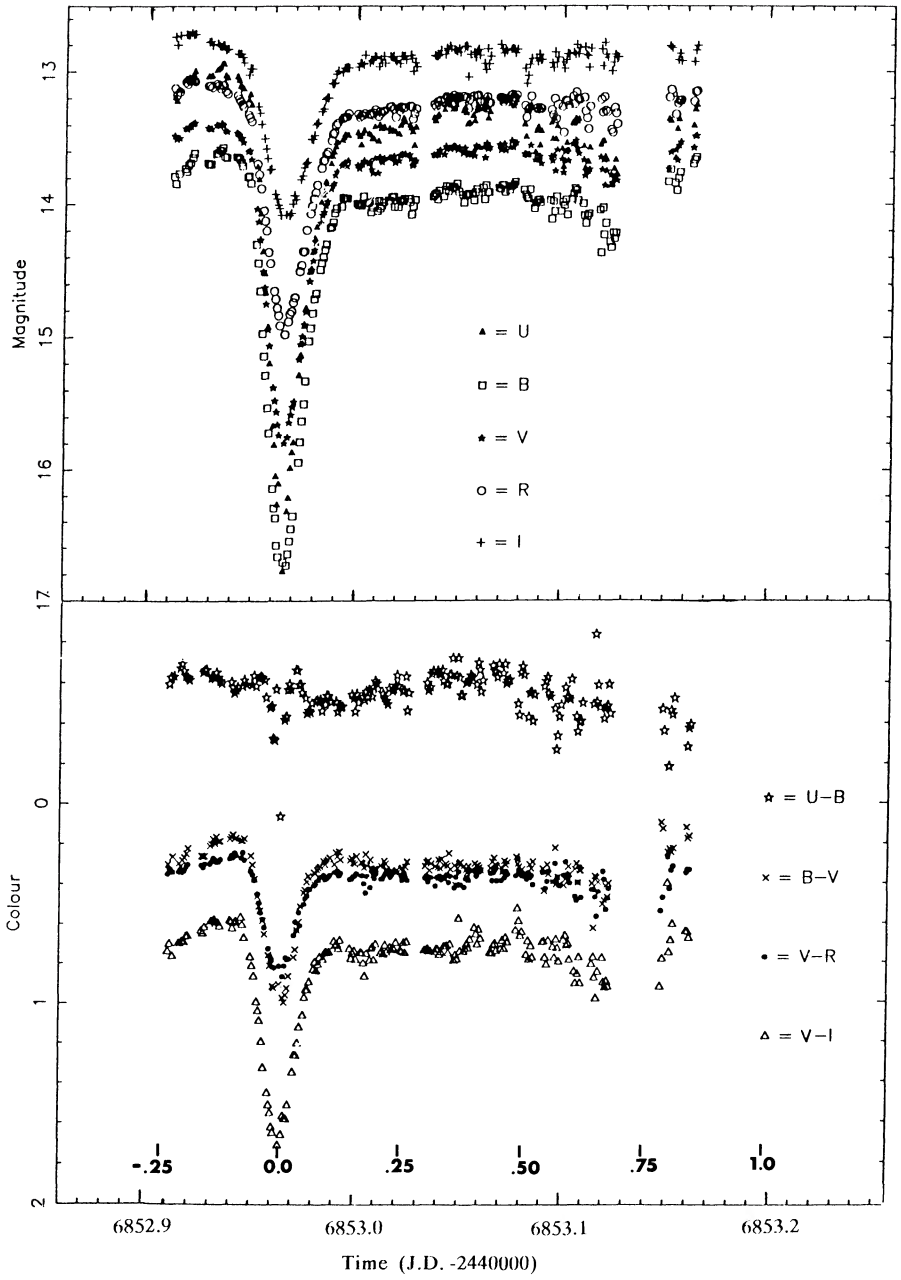

FIG. 10.—*UBVRI* light curve for LB 1800 observed on 1987 February 26 using the 2.3 m ATT telescope at SSO. Tick marks are shown at every 0.25 in orbital phase. The gap in data at phase ~0.75 is due to problems with telescope guiding.

the white dwarf. Angular momentum and energy considerations dictate that the accreted material form a luminous, viscous accretion disk, confined in the orbital plane, which surrounds the white dwarf primary. Emission from this disk is the major luminosity source of the binary, at least in the near-UV–optical regions.

We have determined an accurate photometric period for the system of $0^d.231928$ (5.566 hr), as well as a radial velocity amplitude of 134 km s^{-1} for the Balmer lines, which, following the discussion of § III, we equate to K_{wd}. These results have been used to estimate the secondary mass function for LB 1800. We use

$$f(M_s) = (M_s \sin i)^3/(M_{wd} + M_s)^2 = P_{orb} K_{wd}^3/2\pi G , \quad (1)$$

where the usual symbols are employed, to obtain a mass function of $5.8 \pm 0.3 \times 10^{-2} M_\odot$. Given the usual assumption that the size of the secondary star is constrained by the appropriate critical equipotential surface (Roche lobe), we can use Paczyński's (1971) result for the mean radius, equated to the radius of the secondary star, R_s,

$$R_s/a = 0.462[q/(q + 1)]^{1/3} . \quad (2)$$

We now use the scaled radius formula which relates R_s/a to the inclination, i, and half-width half-depth of the eclipse, $\phi_{1/2}$ (e.g., Penning *et al.* 1984) and is given as

$$(R_s/a)^2 = \cos^2 i + \sin^2 i \sin^2 (2\pi\phi_{1/2}) . \quad (3)$$

The major assumption in the above geometry is that the disk is infinitely thin. Eliminating R_s/a from equations (2) and (3) leads to a determination of the mass ratio, $q = M_s/M_{wd}$, from

$$q/(q+1) = \{[\cos^2 i + \sin^2 i \sin^2 (2\pi\phi_{1/2})]/(0.462)^2\}^{3/2} . \quad (4)$$

The mass function also provides an alternative, dynamical determination of the mass ratio,

$$q/(q+1) = (K_{wd}{}^3 P_{orb}/2\pi G \sin^3 iM_s)^{1/2} . \quad (5)$$

The mass ratio is therefore only dependent on i and M_s, given that the other parameters ($\phi_{1/2}$, K_{wd}, P_{orb}) are observationally constrained. At this point we need an estimate of the secondary mass in order to estimate the inclination, i. In the absence of more direct clues (e.g., the secondary's radial velocity curve), we shall assume that the empirical mass-period relations of Faulkner (1971) and Patterson (1984) are applicable. This implies a secondary mass of $\sim 0.6\ M_\odot$. With this additional estimate, equations (4) and (5) can both provide a model solution for i and q. The best solution is obviously one in which these quantities are the same when derived from the two different equations. It is instructive to explore the solution graphically, and in Figure 11 we show the diagnostic curves derived from these two equations (4) and (5), showing the dependence of orbital inclination on white dwarf mass. The two solid curves are the independent solutions to the two respective equations using the parameter values $P_{orb} = 5.566$ hr, $K_{wd} = 134$ km s^{-1}, $\phi_{1/2} = 0.052$, and $M_s = 0.55\ M_\odot$. Solutions to equation (3) are the more vertically orientated family of curves in Figure 11, while the $\sim 45°$ sloping curves are the solutions to the dynamical equation (4). The combined uncertainties for the parameters P_{orb}, K_{wd}, and $\phi_{1/2}$ result in the dotted curves, which are the limits for the solutions. We find a consistent result for both solutions represented by the shaded overlap region in Figure 11, namely $i > 85°$ and $1.0\ M_\odot < M_{wd} < 1.3\ M_\odot$. This makes LB 1800, interestingly, the highest white dwarf mass system among similar high-excitation eclipsing CVs (e.g., Downes *et al.* 1986).

We now investigate the spatial dimensions of the system which follow from the standard Roche geometry. With $q = 0.46 \pm 0.04$ and $R_s/a = 0.31 \pm 0.01$, the mean radii of the critical equipotential surface of the white dwarf can be estimated from Eggleton's (1983) more accurate expression

$$R_{L1}/a = 0.49q^{-2/3}/[0.6q^{-2/3} + \ln(1 + q^{-1/3})] . \quad (6)$$

This leads to a value of R_{L1}/a of 0.45 ± 0.01 for $q = 0.46 \pm 0.04$. The orbital separation, a, follows directly from Kepler's law:

$$a^3 = G(M_{wd} + M_s)(P_{orb}/2\pi)^2 . \quad (7)$$

We now investigate the size of the accretion disk. We assume that the disk is circular with a radius R_d, is infinitely thin, and is confined to the orbital plane with the white dwarf situated at the center. A lower limit to R_d can be obtained by noting that the eclipse is not total (i.e., not flat-bottomed). Simple geometrical considerations then require

$$[(R_s/a)^2 - \cos^2 i]^{0.5} < R_d/a \Rightarrow \sim 0.31 < R_d/a . \quad (8)$$

Due to the large inclination ($i \geq 85°$), this last result means, in essence, that the disk radius must be larger than the secondary star radius. An *upper* limit for R_d/a of ~ 0.41 then follows from the assumption that a stable disk can exist with a size up to $\sim 90\%$ of the mean radius of the primary Roche lobe (e.g., Shafter, Szkody, and Thorstensen 1986). The orbital inclination will also mean that the farthest point of the disk along the line of sight will be eclipsed at a higher latitude on the secondary's limb. However, for $i > 85°$, this amounts to only $\sim 24°$ for a Roche lobe–filling accretion disk (i.e., $R_d \equiv R_{L1} = 0.45a$), and hence the eclipse duration does not alter much.

An alternative derivation of the outer disk radius relies on the phase of first/last contact and the relationship

$$R_d/a = \sin(2\pi\phi_f) - [(R_s/a)^2 - \cos^2(2\pi\phi_f)\cos^2 i]^{1/2} . \quad (9)$$

The phase of first/last contact is relatively well defined at $\phi_f = 0.105 \pm 0.005$. This leads to an estimate for R_d/a of 0.31 ± 0.02, which is close to the lower limit set above. Thus we conclude that LB 1800 is very close to being a totally eclipsing system.

In Table 4 we present a summary of the best dynamical solution for the LB 1800 system.

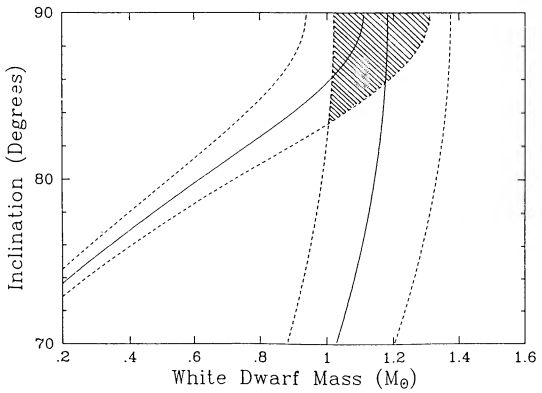

FIG. 11.—Diagnostic inclination–white dwarf mass diagram for LB 1800 from eclipse and radial velocity curve, assuming the empirically determined secondary mass of $0.55\ M_\odot$. The solid curves are the respective eclipse (more vertical lines) and radial velocity (45° lines) constraint solutions for $K = 134$ km s^{-1} and $P = 5.566$ hr, while the dashed lines represent the limits using the quoted uncertainties. The shaded overlap region is the solution "phase space" or domain of consistency.

VII. DISCUSSION AND CONCLUSION

We have shown that the optical counterpart to the transient *HEAO 1* X-ray source 4U 0608−49 is the newly identified bright eclipsing catalysmic variable, LB 1800. This CV exhibits strong emission lines of the high-excitation species He II λ4686 and C III–N III λλ4640–4650, with strengths characteristic of magnetic variables, although spectropolarimetry rules out classification as an AM Her type. The possibility that the

TABLE 4

SYSTEM PARAMETERS FOR LB 1800

Parameter	Value
i	$87° \pm 3°$
M_{wd}	$1.2 \pm 0.1\ M_\odot$
M_s[a]	$0.55\ M_\odot$
q	0.46 ± 0.04
a	$1.91 \pm 0.05\ R_\odot$
R_s	$0.60 \pm 0.03\ R_\odot$
R_d	$0.60 \pm 0.06\ R_\odot$
P	5.566 hr
K	134 ± 9 km s^{-1}
$f(M_s)$	$5.8 \pm 0.3 \times 10^2\ M_\odot$

[a] From Patterson's 1984 empirical M_s–period relation.

system is a DQ Her, or intermediate polar, system is speculative though perhaps supported by the large L_x/L_{opt} ratio (~ 4). Interestingly, Williams (1989) has raised the possibility that many high-excitation nova-likes are hitherto unrecognized magnetic CVs. He bases this assertion upon the problems in reconciling the observed emission-line profiles with those calculated for undisrupted accretion disks. The possibility that LB 1800 might be an intermediate polar will be resolved in the future by searching for coherent optical pulsations.

The equivalent widths for the lines Hα, Hβ, and He II λ4686, plotted against the orbital inclination, all cluster near the loci for nova remnants (Warner 1986). Furthermore, from Warner's (1986) $M_v - i$ correlation, we derive an estimate for the absolute magnitude of LB 1800 ranging from $M_v \sim 5.3$–7.0. This in turn leads to a distance for LB 1800 in the range 174–380 pc, based on the observed out-of-eclipse magnitude of $V \sim 13.4$ and a $E(B-V) < 0.06$, the latter an upper limit based on the Galactic latitude of LB 1800 ($b \sim -27°$). The implied 2–10 keV luminosity is therefore between $\sim 2 \times 10^{32}$ and 1.3×10^{33} ergs cm^{-2} s^{-1}.

LB 1800 exhibits deep eclipses (~ 3 mag in U) which are morphologically similar to other high-excitation nova-like eclipsing CVs. The often double-peaked emission lines are shown to consist of red and blue peaks which alter in relative intensity over the orbital cycle. This behavior is thought to be due to the varying visibility of a disk hot spot (i.e., s-wave). The double peaks may be a result of an absorption self-reversal, rather than a dynamical splitting, since the dip between the peaks is seen to be wavelength-dependent among the Balmer series lines. Furthermore, the greatest depth of this supposed absorption reversal occurs when the Ca II H and K absorption lines are most noticeable, and this occurs at an orbital phase when the cool accretion stream from the secondary is seen projected against the bright disk. The system has an orbital period of ~ 5.6 hr, making it the fifth longest period eclipsing CV system (e.g., Ritter 1984). The eclipse widths of both the continuum and emission lines are equal, indicating that the respective emission regions have a similar *radial* extent. The possibility therefore exists that the emission line region is extended in the *vertical* direction, i.e., an optically thick disk is overlaid by a vertically extended, optically thinner "chromosphere."

The dynamical and eclipse solutions for LB 1800 indicate that the inclination is probably in the region 87° for an empirically derived secondary mass of 0.55 $M_\odot$. Even if the secondary is undermassive, as is conventionally thought, the inclination is still $> \sim 80°$. The estimate for the white dwarf mass of $\sim 1.2\ M_\odot$ is interestingly high, compared to the masses of other similar systems. From an analysis of the light curve, we have derived an estimate of the accretion disk size which is only marginally larger than the occulting secondary. In many respects LB 1800 resembles other high-excitation eclipsing nova-like systems (e.g., SW Sex, V1315 Aql, and DW UMa); however, it is different in respect to how well behaved the radial velocity curve is in comparison to those of other systems. In particular, the continuum and line eclipses are exactly in phase and coincide with the radial velocity zero crossing phase (superior conjunction).

Work in progress on LB 1800 will address the accretion disk line profiles derived from recently obtained spectroscopy and second epoch photometry.

We wish to acknowledge John Norris (MSSO) for his part in the initial serendipitous discovery of LB 1800 as a CV. Jeremy Bailey (AAO) kindly undertook the spectropolarimetry measurements. D. J. S. wishes to thank the Physics Department, University of Canterbury, for the allocation of MJUO observing time and acknowledges financial support from the N.Z. University Grants Committee. Some of this work was carried out while D. J. S. was a Visiting Fellow at MSSSO. We are grateful to Professor Alex Rodgers, Director of MSSSO, for being given unscheduled 1.9 m telescope time. Thanks to Wendy Roberts (SAO/CfA) and Drummond Laing (SAAO) for producing two of the figures. D. A. H. B. acknowledges support by an ANU Post-Graduate Scholarship. Also, R. R. acknowledges NASA grant NAG 8-493 and NSF grant AST 86-12572.

REFERENCES

Cook, M. C., and Warner, B. 1984, *M.N.R.A.S.*, **207**, 705.
Córdova, F., and Mason, K. O. 1984, *M.N.R.A.S.*, **206**, 879.
Downes, R. A., Mateo, M., Szkody, P., Jenner, D. C., and Margon, B. 1986, *Ap. J.*, **301**, 240.
Eggleton, P. P. 1983, *Ap. J.*, **268**, 368.
Faulkner, J. 1971, *Ap. J. (Letters)*, **170**, L99.
Forman, W., *et al.* 1978, *Ap. J. Suppl.*, **38**, 357.
Gursky, H., *et al.* 1978, *Ap. J.*, **223**, 973.
Honeycutt, R. K., Schlegel, E. M., and Kaitchuck, R. H. 1986, *Ap. J.*, **302**, 388.
Horne, K. 1985, *M.N.R.A.S.*, **213**, 129.
Horne, K., and Steining, R. F. 1985, *M.N.R.A.S.*, **216**, 933.
Horne, K., Wade, R. A., and Szkody, P. 1986, *Ap. J.*, **219**, 791.
Kaitchuck, R. H., Honeycutt, R. K., and Schlegel, E. M. 1983, *Ap. J.*, **267**, 239.
Luyten, W. J., and Anderson, J. H. 1958, *A Search for Faint Blue Stars XII* (Minneapolis: University of Minnesota).
Mason, K. O. 1985, *Space Sci. Rev.*, **40**, 99.
O'Donoghue, D., Fairall, A. P., and Warner, B. 1987, *M.N.R.A.S.*, **225**, 43.
Paczyński, B. 1971, *Ann. Rev. Astr. Ap.*, **9**, 183.
Patterson, J. 1984, *Ap. J. Suppl.*, **54**, 443.
Patterson, J., and Raymond, J. C. 1985, *Ap. J.*, **292**, 535.
Penning, W. R., Ferguson, D. H., McGraw, J. T., and Leibert, J. 1984, *Ap. J.*, **276**, 233.
Pringle, J. E., and Savonije, G. J. 1979, *M.N.R.A.S.*, **187**, 777.
Remillard, R. A., Bradt, H. V., Buckley, D. A. H., Roberts, W., Schwartz, D. A., Tuohy, I. R., and Wood, K. 1986, *Ap. J.*, **301**, 742.
Ritter, H. 1984, *Astr. Ap.*, **57**, 385.
Rodgers, A. W., van Harmalen, J., King, D., Conroy, P., and Harding, P. 1988, *Pub. A.S.P.*, **100**, 841.
Schneider, D. P., and Young, P. 1980, *Ap. J.*, **238**, 946.
Shafter, A. W. 1983, PhD. thesis, UCLA.
———. 1985, in *Cataclysmic Variables and Low Mass X-Ray Binaries*, ed. D. Q. Lamb and J. Patterson (Dordrecht: Reidel), p. 355.
Shafter, A. W., Hessman, F. V., and Zhang, E. H. 1988, *Ap. J.*, **327**, 248.
Shafter, A. W., Szkody, P., and Thorstensen, J. R. 1986, *Ap. J.*, **308**, 765.
Stapinski, T. E., Rodgers, A. W., and Ellis, M. J. 1981, *Pub. A.S.P.*, **93**, 242.
Sulkanen, M. E., Brasure, L. W., and Patterson, J. 1981, *Ap. J.*, **244**, 579.
Tonry, J., and Davis, M. 1979, *A.J.*, **84**, 1511.
Tylenda, R. 1981, *Acta Astr.*, **31**, 267.
van der Peet, A. J. 1987, MSc thesis, Victoria University of Wellington.
Warner, B. 1986, *M.N.R.A.S.*, **222**, 11.
Warner, B., and Cropper, M. 1983, *M.N.R.A.S.*, **203**, 909.
Warner, B., and O'Donoghue, D. 1987, *M.N.R.A.S.*, **224**, 733.
———. 1988, *M.N.R.A.S.*, **233**, 705.
Watts, D. J., Bailey, J., Hill, P. W., Greenhill, J. G., McCowage, C. and Carty, T. 1986, *Astr. Ap.*, **154**, 197.
Williams, R. E. 1989, *A.J.*, submitted.
Wood, J., Irwin, M., and Pringle, J. E. 1985, *M.N.R.A.S.*, **214**, 475.
Wood, K., *et al.* 1984, *Ap. J. Suppl.*, **56**, 507.
Zhang, E. H., Robinson, E. L., and Nather, R. E. 1986, *Ap. J.*, **305**, 740.

D. A. H. BUCKLEY: Astronomy Department, University of Cape Town, Private Bag, Rondebosch 7700, Cape Town, South Africa

M. CLARK: Mount John University Observatory, P.O. Box 52, Lake Tekapo, New Zealand

R. A. REMILLARD: Center for Space Research, Massachusetts Institute of Technology, Room 37-595, Cambridge, MA 02139

D. J. SULLIVAN: Physics Department, Victoria University of Wellington, Private Bag, Wellington, New Zealand

I. R. TUOHY: British Aerospace Australia, P.O. Box 180, Salisbury, S.A. 5108, Australia